hepatic vein evaluation with spiral CT. *Radiology* 1997;202;715-720.

13) Murata S, Tajima H, Abe Y, et al. Temporary occlusion of two hepatic veins for chemoembolization of hepatocellular carcinoma with arteriohepatic vein shunts. *AJR* 2005;184:415-418.

14) Itai Y, Moss AA, Goldberg HI. Transient attenuation difference of lobar or segmental distribution detected by dynamic computed tomography. *Radiology* 1982;144(4):835-839.

15) Mathieu D, Vasile N, Grenier P. Portal thrombus: dynamic CT features and course. *Radiology* 1985;154:737-741.

16) Irie T, Terahata S, Hatsuse K, et al. Postsurgical intrahepatic portal thromboembolism: a possible cause of perfusion defects on CT during arterial portography. *J Comput Assist Tomogr* 1995;19:204-210.

17) Matsui O, Takashima T, Kadoya M, et al. Segmental staining on hepatic arteriography as a sign of intrahepatic portal vein obstraction. *Radiology* 1984;152:601-606.

18) Itai Y, Ohtomo K, Kokubo T, Okada Y, Yamauchi T, Yoshida H. Segmental intensity differences of the liver on MR images: a sign of intrahepatic portal flow stoppage. *Radiology* 1988;167:17-19.

19) Itai Y, Murata S, Kurosaki Y. Straight border sign of the liver: spectrum of CT appearances and causes. *RadioGraphics* 1995;15:1089-1102.

20) Itai Y, Matsui O. Blood flow and liver imaging. *Radiology* 1997;202:306-314.

21) Lautt WW, Legare DJ, Ezzat WR. Quantitation of the hepatic arterial buffer response to graded changes in portal blood flow. *Gastroenterology* 1990;98:1024-1028.

22) Rocheleau B, Ethier C, Houle R, Huet PM, Bilodeau M. Hepatic artery buffer response following left portal vein ligation: its role in liver tissue homeostasis. *Am J Physiol Gstrointest Liver Physiol* 1999;277:G1000-1007.

23) Mucke I, Richter S, Menger MD, Vollmar B. Significance of hepatic arterial responsiveness for adequate tissue oxygenation upon portal vein occlusion in cirrhotic liver. *Int J Colorectal Dis* 2000;15:335-341.

24) Kan Z, Ivancev K, Hagerstrand I, Chuang VP, Lunderquist A. In vivo microscopy of the liver after injection of Lipiodol into the hepatic artery and portal vein in the rat. *Acta Radiol* 1989;30:419-25.

25) Kan Z, Sato M, Ivancev K, et al. Distribution and effect of iodized poppyseed oil in the liver after hepatic artery embolization: experimental study in several animal species. *Radiology* 1993;186:861-866.

26) Kan Z, Ivancev K, Lunderquist A. Peribiliary plexa-important pathways for shunting of iodized oil and silicon rubber solution from the hepatic artery to the portal vein. An experimental study in rats. *Invest Radiol* 1994;29:671-676.

27) Murata S, Ivancev K, Jeppsson B, Lunderquist A. Hemodynamic changes in the liver during complete hepatic venous occlusion: applicability in treatment of hepatic malignancy (abst). *CVIR* 1998;99(S):116.

Management of Pancreaticoduodenal Artery Aneurysms: Results of Superselective Transcatheter Embolization

Satoru Murata[1]
Hiroyuki Tajima[1]
Tsuyoshi Fukunaga[1]
Yutaka Abe[1]
Pascal Niggemann[2]
Shiro Onozawa[1]
Tatsuo Kumazaki[1]
Masayuki Kuramochi[3]
Kemmei Kuramoto[4]

OBJECTIVE. The purpose of our study was to assess the efficacy of transcatheter arterial embolization for pancreaticoduodenal artery aneurysms.

CONCLUSION. We concluded that transcatheter arterial embolization is the initial and definitive therapeutic choice for pancreaticoduodenal artery aneurysms, with a possible option to perform surgery after embolization.

Keywords: aneurysm, embolization, interventional radiology, pancreas

DOI:10.2214/AJR.04.1726

Received November 9, 2004; accepted after revision May 19, 2005.

[1]Department of Radiology, Nippon Medical School, 1-1-5 Sendagi, Bunkyou-ku, Tokyo, Japan 113-8602. Address correspondence to S. Murata.

[2]Department of Radiology, RWTH Aachen University Hospital, Aachen, Germany.

[3]Department of Radiology, Hitachi General Hospital, Hitachi, Ibaragi, Japan.

[4]Department of Diagnostic Radiology, National Disaster Medical Center, Tokyo, Japan.

WEB
This is a Web exclusive article.

AJR 2006; 187:W290–W298

0361–803X/06/1873–W290

© American Roentgen Ray Society

Aneurysms of the pancreaticoduodenal arteries are rare and make up only 2% of all splanchnic aneurysms [1]. Pancreaticoduodenal artery aneurysms may have an increased propensity for rupture: 64% of patients seeking medical advice from symptoms related to the aneurysm have had a rupture [2]. Pancreaticoduodenal artery aneurysm ruptures can be life threatening because they result in bleeding into the retroperitoneal space, abdominal cavity, the gastrointestinal tract, or a combination of these. Before 1980, surgery was the only treatment for pancreaticoduodenal artery aneurysm, and its mortality rate was 26% [3]. However, the in-hospital mortality rate for patients who received no surgical treatment was 80% [3].

Recently, the rapid development of interventional radiology has made it possible to perform transcatheter arterial embolization of visceral aneurysms safely and effectively. In addition to surgery, transcatheter arterial embolization has been performed since 1980, and the mortality rate has significantly improved [3–4]. Despite these facts, the choice of initial therapy remains controversial.

During the last decade, the number of case reports of pancreaticoduodenal artery aneurysm has increased because of improved detection rates with advances in noninvasive diagnostic techniques, such as CT and sonography. Therefore, it is important to choose a therapy—transcatheter arterial embolization or surgery—for initial treatment. The purposes of this article are to evaluate the results of transcatheter arterial embolization therapy and to discuss which treatment should be chosen for pancreaticoduodenal artery aneurysms in various cases.

Subjects and Methods

Patients

Between January 1992 and December 2002, 10 patients with pancreaticoduodenal artery aneurysms were admitted to Nippon Medical School Hospital. The clinical findings of these patients are summarized in Table 1. One woman and nine men, with a median age of 57 years (range, 45 to 72 years) were identified. All patients underwent transcatheter arterial embolization. Three patients had a history of hypertension and three were alcoholics. Two patients had a history of partial gastrectomy for gastric ulcer, and one of them showed signs of ileus. One patient had advanced common bile duct cancer. One patient had no history of any particular disease. Nine of the 10 patients had ruptured pancreaticoduodenal artery aneurysms. Five of these nine had gastrointestinal bleeding, and two also had hematemesis. Six patients were hemodynamically stable during and after volemic resuscitation, but three were hemodynamically unstable (shock index: heart rate/systolic blood pressure > 1) despite volemic resuscitation. One of those with shock received emergency laparotomy, and the other two underwent clipping by endoscopy with the intention of stopping the bleeding before embolization; however, in these three patients the bleeding could not be stopped. They therefore required immediate embolization. The patient whose aneurysm had not ruptured was symptom free. She was followed up by her family physician, and CT revealed that the aneurysm increased in diameter from 2 to 2.8 cm within 1 year. She rejected surgical resection after the surgeons explained the potential complications of surgery, and she decided to undergo transcatheter arterial embolization.

TABLE 1: Summary of Patient Data

Patient No./Age (y)/Sex	Clinical Symptom	Medical History	Location of Aneurysm	Diameter of Aneurysm (mm)	Rupture	Approach Route	Embolization Technique			Technical Success	30-Day Clinical Success	Outcome
							Afferent	Packing	Efferent			
1/72/F[a]	None	CAS	IPDA	28	No	Both[e]	Done	None	Done	Yes	Yes	Survival
2/54/M[a]	Abdominal pain	CAS	IPDA IPDA	33 7	Yes	SMA	Done Done	Done Done	None None	Yes Yes	Yes	Survival
3/58/M[a]	Abdominal pain Shock	CAO MALS	IPDA	32	Yes	SMA	Done	None	None	Yes	No	Survival
4/48/M[b]	Abdominal pain	Pancreatitis	IPDA	23	Yes	SMA	Done	None	Done	Yes	Yes	Survival
5/53/M	Abdominal pain	Unknown	IPDA IPDA ASPDA 1st jejunal	9 7 6 4	Yes Yes Yes No	Both[e]	Done Done Done Done	None[f] None[f] None[f] Done	Done Done Done None	Yes Yes Yes	Yes	Survival
6/45/M[c]	Shock Hematemesis	PG Gastric ulcer	IPDA	7	Yes	SMA	Done	Done	None	Yes	Yes	Survival
7/53/M[d]	Shock Ileus Peritonitis	PG Gastric ulcer	ASPDA	5	Yes	Celiac artery	Done	Done	None	Yes	No[g]	Death
8/70/M[d]	Hematemesis Melena	CBD cancer	IPDA	5	Yes	Celiac artery	Done	Done	None	Yes	Yes	Survival
9/62/M[b]	Melena	Pancreatitis	IPDA	8	Yes	Both[e]	Done	None	Done	Yes	Yes	Survival
10/57/M[b]	Melena	Pancreatitis	IPDA	6	Yes	Celiac artery	Done	None	Done	Yes	Yes	Survival

Note—CAS = celiac axis stenosis, IPDA = inferior pancreaticoduodenal artery, SMA = superior mesenteric artery, CAO = celiac axis occlusion, MALS = median arcuate ligament syndrome, ASPDA = anterior superior pancreaticoduodenal artery, PG = partial gastrectomy, CBD = common bile duct.

[a]Hypertension.

[b]Alcoholism.

[c]Emergency laparotomy before transcatheter arterial embolization.

[d]Endoscopic treatment before transcatheter arterial embolization.

[e]Both the SMA and celiac artery routes were used.

[f]Transcatheter arterial embolization using gelatin sponge.

[g]Patient had surgery after embolization for failure of sutures and then suffered disseminated intervascular coagulation.

Embolization Technique

After diagnostic angiography with a 5-French catheter, a 3-French microcatheter was inserted as close as possible to the aneurysm. Arteriography was then performed.

The method of embolization of the pancreaticoduodenal artery aneurysm was as follows: The basic procedure involved isolation and exclusion of the afferent and efferent arteries close to the aneurysm, using microcoils with a coaxial system to exclude and occlude the aneurysm because of the presence of anastomotic branches around the pancreas. If a microcatheter could not be advanced into the efferent arteries, we first tried to pack the aneurysm and then embolized the afferent arteries with microcoils. If a microcatheter could not be advanced into the aneurysm (i.e., if we could not even pack the aneurysm), we embolized the afferent arteries and recommended surgical treatment.

Informed consent for embolization was obtained from conscious patients as far as the emergency permitted. Otherwise, the immediate family was informed.

Data Analysis

Technical success reflects immediate results and is typically evaluated by completion angiography [5]. The technical success of our series was defined as nonvisualization of aneurysms and nonvisualization of bleeding, as verified by postembolization angiography. Clinical success reflects the results in the 30 days immediately after the embolization procedure and is typically assessed by close patient follow-up [5]. Clinical success in our series was defined by the patients' condition (the 30-day outcome)—that is, whether patients were hemodynamically stable without blood transfusion. Cases in which additional surgery or endoscopic treatment for the aneurysm were performed after the embolization procedure were excluded from the clinical successes. For follow-up, contrast-enhanced CT or sonography was performed in each patient 1 week to 2 months after embolization to assess the stoppage of bleeding or thrombosis of the aneurysms or both. In particular, patients with celiac trunk stenosis ($n = 2$) were given an additional follow-up contrast-enhanced CT every 3 months for 1 year, and every 6 months after 1 year (range, 21 months to 34 months; mean, 27.5 months) to check for the presence of recurrent or new aneurysms.

Results

The causes of these pancreaticoduodenal artery aneurysms were arteriosclerosis, in association with celiac axis stenosis or occlusion ($n = 2$); compression of the median arcuate ligament of the diaphragm ($n = 1$); pancreatitis ($n = 3$); postsurgery ($n = 2$); advanced common bile duct cancer ($n = 1$); and unknown ($n = 1$) (patient had no history of systemic vascular disease, abdominal trauma, or chronic pancreatitis).

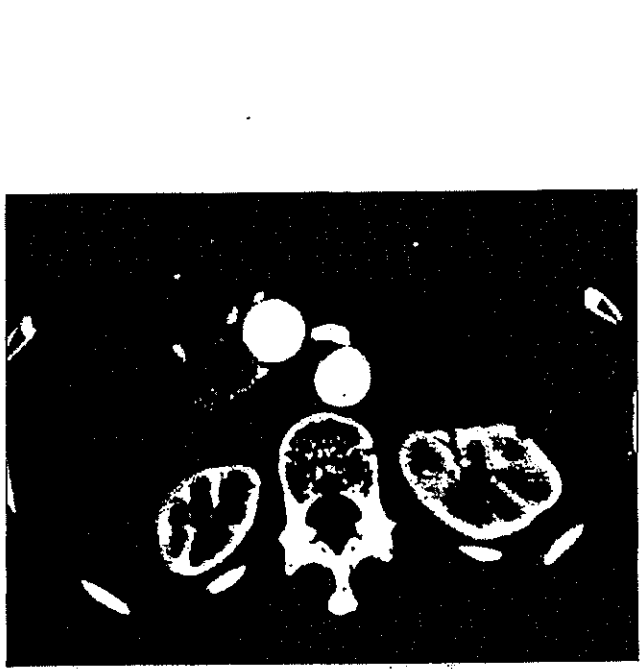

A

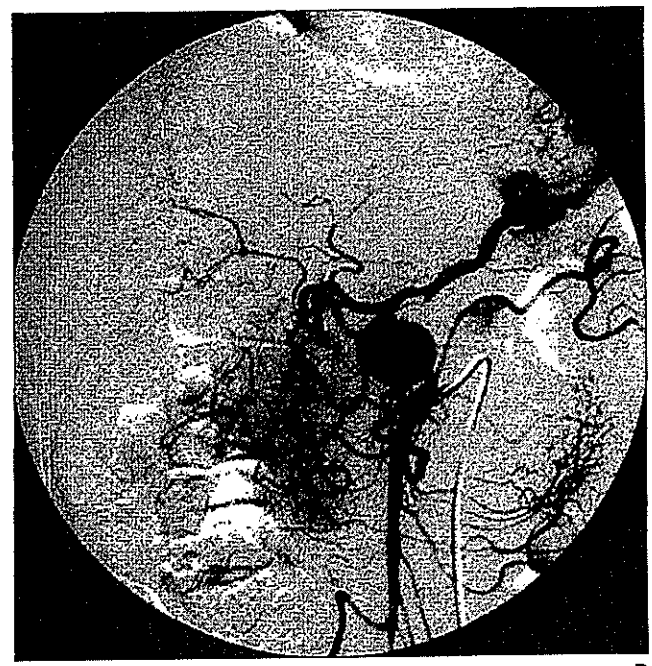

B

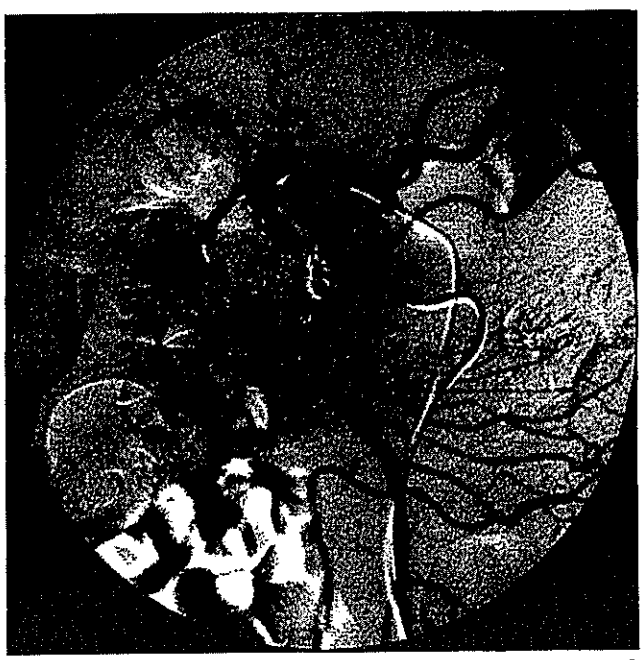

C

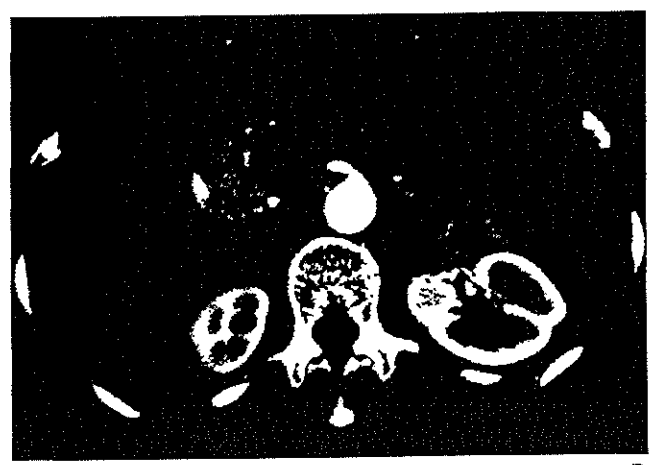

D

Fig. 1—72-year-old woman with embolization of nonruptured pancreaticoduodenal artery aneurysm caused by celiac axis stenosis.
A, Contrast-enhanced CT scan reveals aneurysm (2.8 cm in diameter) located behind pancreas head.
B, Angiography of superior mesenteric artery shows pancreaticoduodenal artery aneurysm of inferior pancreaticoduodenal artery. Hepatic arteries and splenic artery are opacified through dilated dorsal pancreas artery as main feeder. Afferent artery of aneurysm is embolized through superior mesenteric artery route, and efferent artery is also embolized through celiac artery route.
C, Superior mesenteric arteriography after embolization of aneurysm shows no visualized aneurysm.
D, Contrast-enhanced CT scan 1 week after transcatheter arterial embolization shows complete thrombosis of the aneurysm.

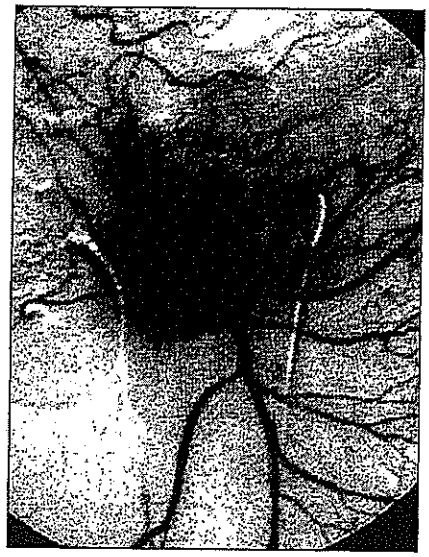

A

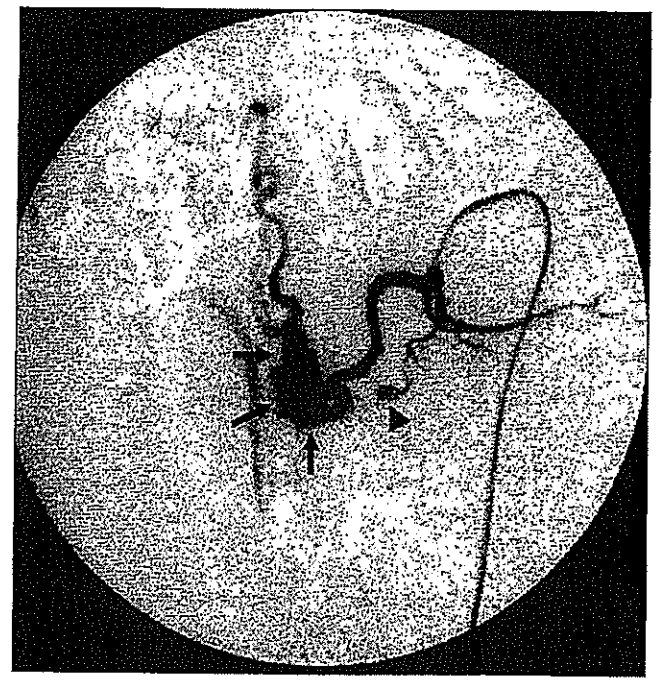

B

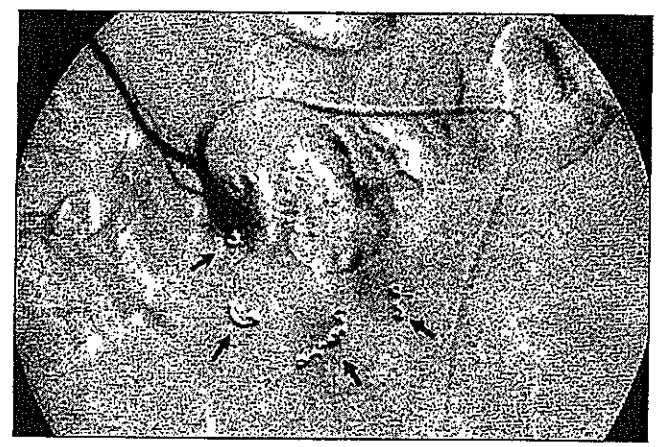

C

Fig. 2—53-year-old man with embolization of multiple ruptured pancreaticoduodenal artery aneurysms.
A, Superior mesenteric arteriogram shows four aneurysms.
B, Selective inferior pancreaticoduodenal arteriogram clearly shows aneurysms, three on the pancreaticoduodenal artery (*arrows*) and one on first jejunum artery (*arrowhead*).
C, Gastroduodenal artery arteriogram after embolization with microcoils (*arrows*) and gelatin sponge particles shows no extravasation and no visualized aneurysms.

Angiographic and CT Findings

Angiography revealed 13 pancreaticoduodenal artery aneurysms ranging from one to three in each patient, and the sizes of the aneurysms ranged from 5 to 33 mm (median, 13.5 mm). Eleven of the 13 aneurysms were located in the inferior pancreaticoduodenal artery, and the remaining two were in the anterior superior pancreaticoduodenal artery. Bleeding from the aneurysm was recognized in four patients on angiography, and true aneurysms were recognized in four patients (celiac stenosis or occlusion, $n = 3$; unknown, $n = 1$) by angiographic findings. Evaluation by CT was performed in eight of 10 patients before angiography, which showed intraabdominal hematoma in six patients. One of the remaining two patients who did not undergo CT was found by angiography to have intraabdominal bleeding.

Technical Success

Nine of the 10 patients with pancreaticoduodenal artery aneurysms were successfully embolized by transcatheter arterial embolization alone using only microcoils (eight patients) or using microcoils combined with gelatin sponge (one patient). In five of the 10 patients, isolation was obtained with microcoils using the coaxial system to exclude both afferent and efferent arteries close to the aneurysm. Of these five patients, one had an unruptured aneurysm, seen with CT and Doppler sonography, 1 week after embolization. The patient was found to have complete thrombosis of the aneurysm (Fig. 1). In another patient, we had intended to perform the isolation using only microcoils, but we did not have enough microcoils on hand. Consequently, we first embolized the inferior pancreaticoduodenal artery and a small

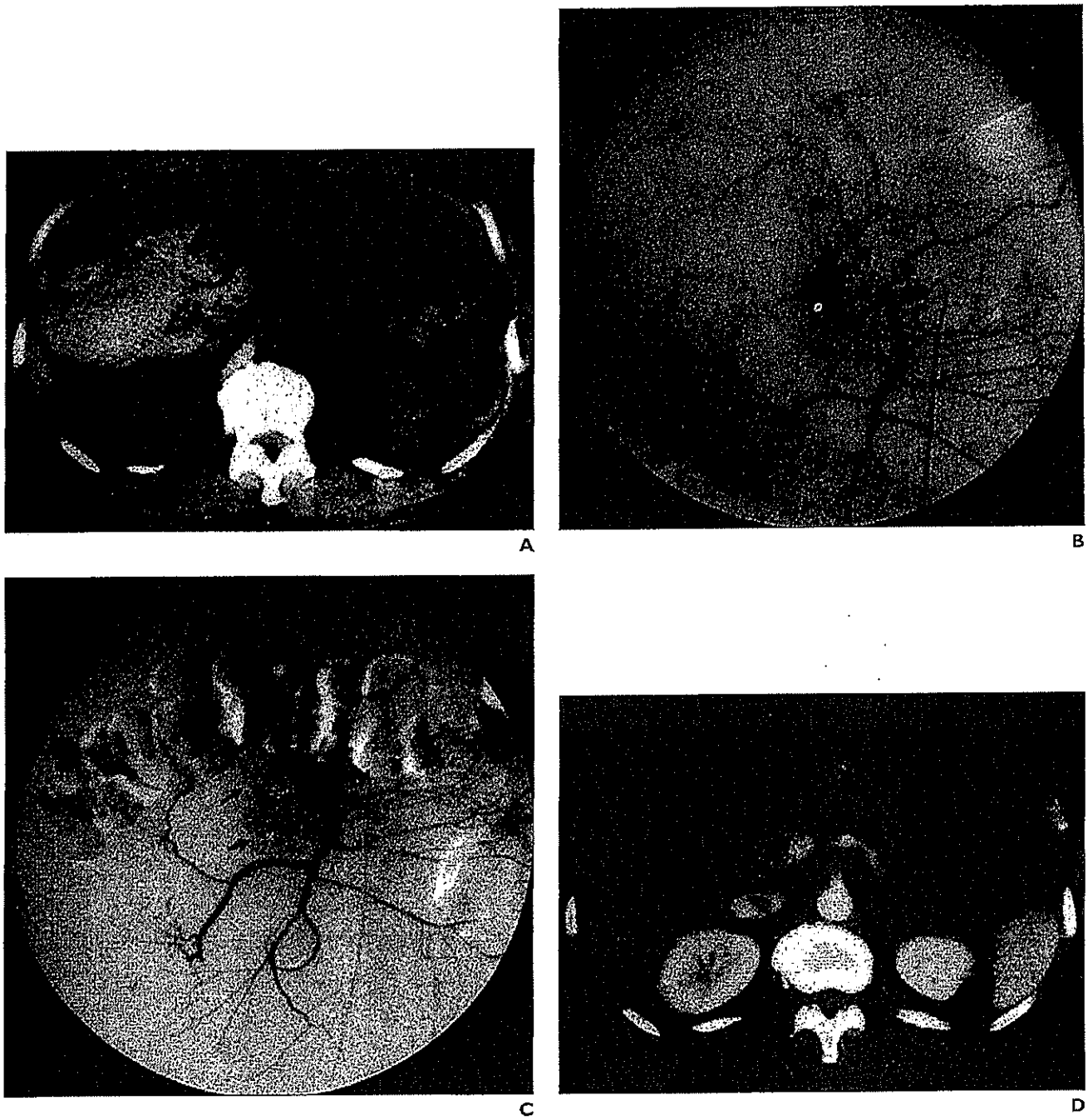

Fig. 3—54-year-old man with embolization of ruptured pancreaticoduodenal artery aneurysms caused by celiac axis stenosis.
A, Unenhanced CT scan shows retroperitoneal hematoma.
B, Selective superior mesenteric arteriogram shows two aneurysms, 3.3 cm and 0.5 cm in diameter, arising from anterior inferior pancreaticoduodenal artery.
C, Selective superior mesenteric arteriogram after embolization with microcoils (*arrows*) shows no visualized aneurysms.
D, Contrast-enhanced CT scan 4 weeks after embolization shows no hematoma in abdominal cavity.

aneurysm of the first jejunal artery with microcoils, and then embolized the superior pancreaticoduodenal artery with particles of gelatin sponge. After these procedures, the superior pancreaticoduodenal artery was embolized with microcoils (Fig. 2). Four patients underwent packing of their aneurysms and embolization of the afferent arteries with microcoils (Fig. 3). In the remaining patient, who had rup-

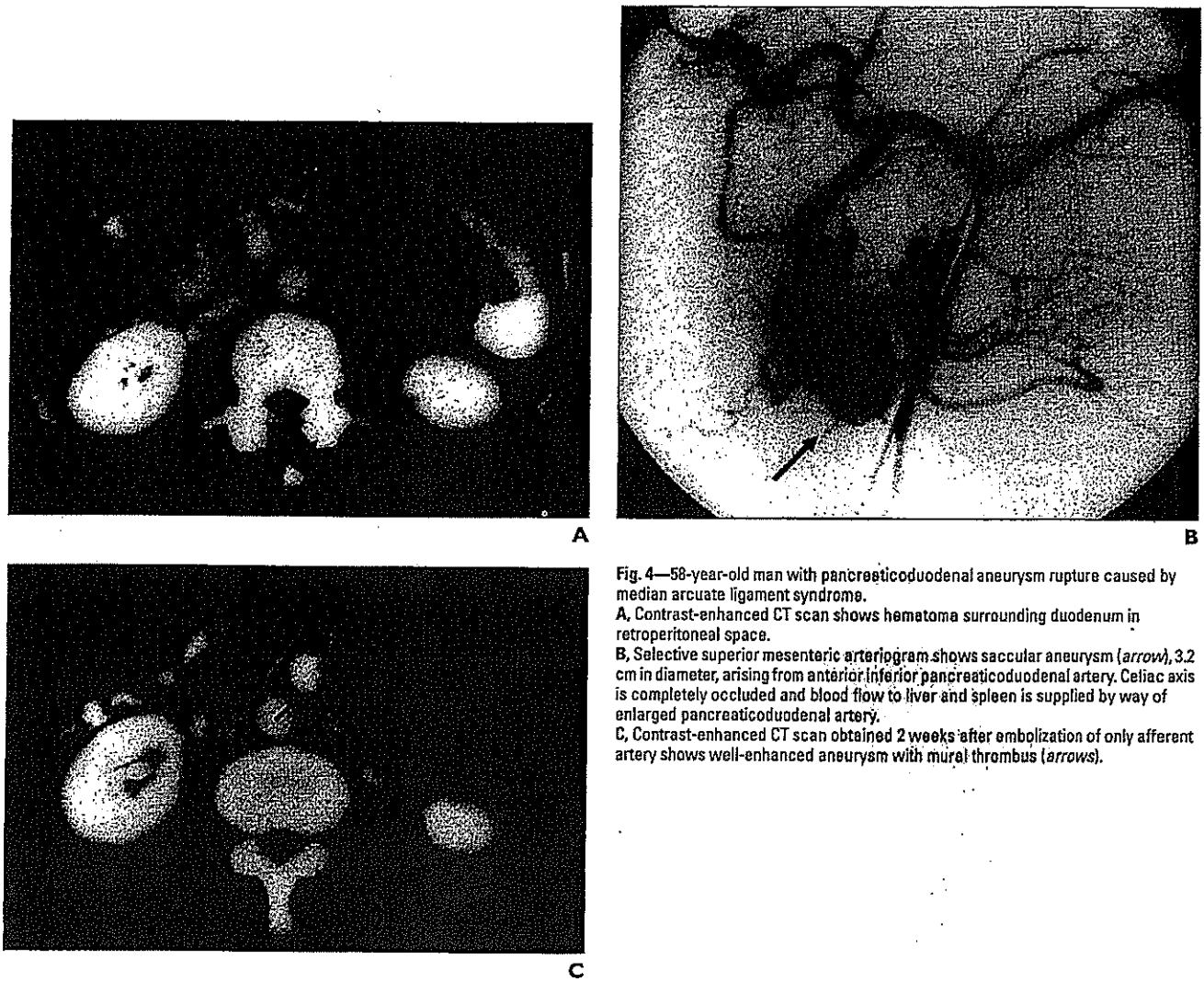

Fig. 4—58-year-old man with pancreaticoduodenal aneurysm rupture caused by median arcuate ligament syndrome.
A, Contrast-enhanced CT scan shows hematoma surrounding duodenum in retroperitoneal space.
B, Selective superior mesenteric arteriogram shows saccular aneurysm (*arrow*), 3.2 cm in diameter, arising from anterior inferior pancreaticoduodenal artery. Celiac axis is completely occluded and blood flow to liver and spleen is supplied by way of enlarged pancreaticoduodenal artery.
C, Contrast-enhanced CT scan obtained 2 weeks after embolization of only afferent artery shows well-enhanced aneurysm with mural thrombus (*arrows*).

ture of the pancreaticoduodenal artery aneurysm caused by compression of the median arcuate ligament, although we managed to advance a microguidewire into the aneurysm, a microcatheter could not be advanced along with the microguidewire because of the tortuous nature of the afferent artery and the use of an initial coaxial catheter system. Therefore, we embolized only the afferent artery with microcoils (Fig. 4). Superior mesenteric arteriography immediately after embolization showed no visible aneurysm, and the patient became hemodynamically stable. We recommended surgery because we considered him to be at high risk for re-rupture, but he rejected surgery.

The technical success rate of embolization as an immediate result was 100% (10 of 10 patients).

Clinical Success

There were no complications directly resulting from the embolization procedures and no cases of re-rupture. We observed two instances in which we did not obtain clinical success between days 8 and 14. One patient was successfully treated by embolization of the ruptured pancreaticoduodenal artery aneurysm (Fig. 5) and became hemodynamically stable. He then received repeat surgery for suture failure 3 days after embolization but developed disseminated intervascular coagulation and died 5 days after the repeat surgery. The other patient was treated by embolization of only the afferent artery with microcoils (Fig. 4); he was hemodynamically stable after transcatheter arterial embolization and rejected surgery. A follow-up contrast-enhanced CT at 14 days after transcatheter arterial embolization, however, showed a well-enhanced pancreaticoduodenal artery aneurysm. Therefore, he agreed to undergo surgery, and surgical treatment was successfully performed.

The other eight patients were stable after transcatheter arterial embolization and were discharged from the hospital. Use of CT at 1 or 2 months after embolization showed diminished intraabdominal hematoma in five of five patients. As we could not obtain clinical success in two patients, the clinical success rate was 80% (8 of 10 patients). The mortality rate with transcatheter arterial embolization for pancreaticoduodenal artery aneurysms was 0%. Two patients with celiac trunk stenosis had no recurrent or new aneurysms (fol-

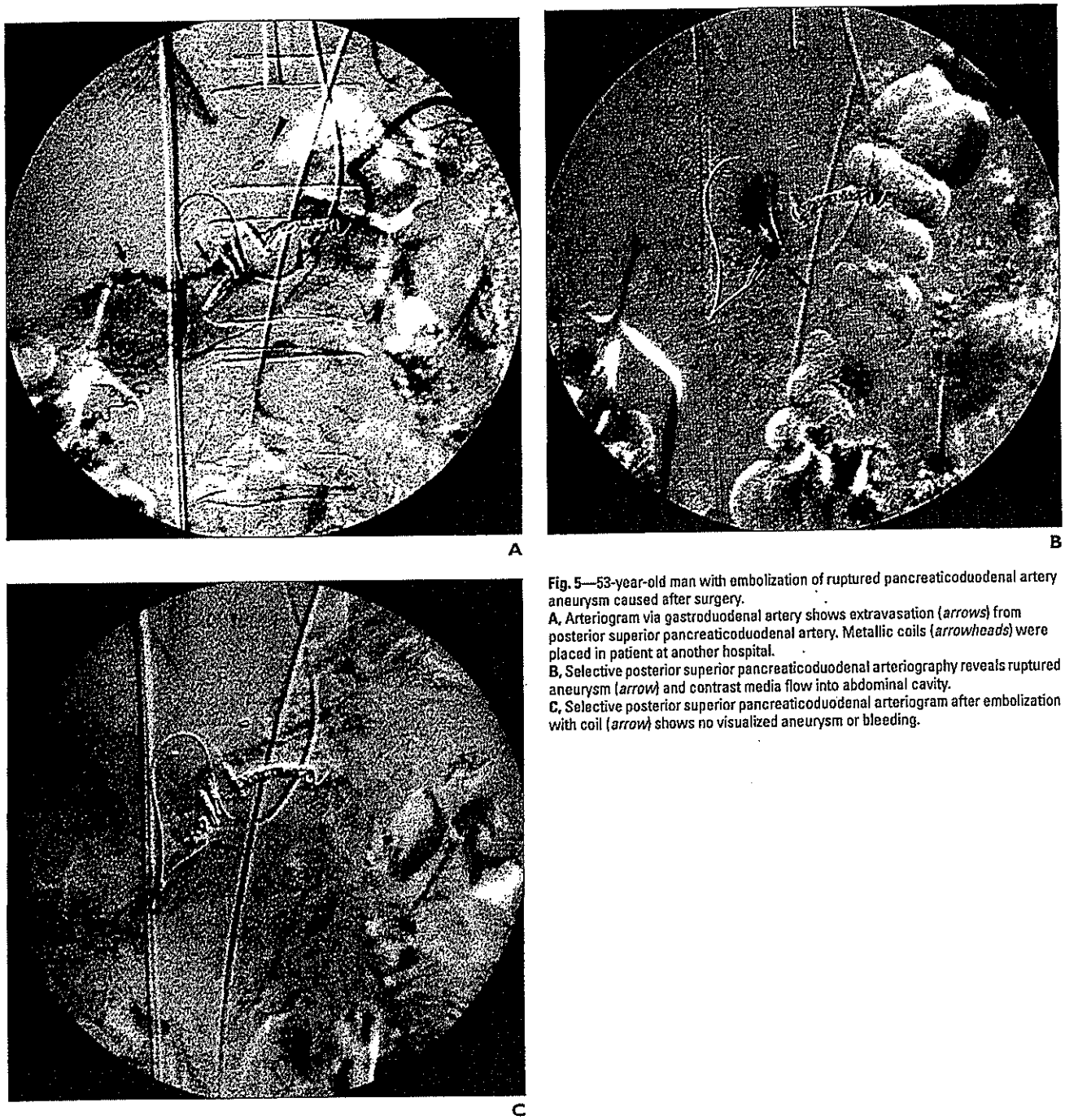

Fig. 5—53-year-old man with embolization of ruptured pancreaticoduodenal artery aneurysm caused after surgery.
A, Arteriogram via gastroduodenal artery shows extravasation (*arrows*) from posterior superior pancreaticoduodenal artery. Metallic coils (*arrowheads*) were placed in patient at another hospital.
B, Selective posterior superior pancreaticoduodenal arteriography reveals ruptured aneurysm (*arrow*) and contrast media flow into abdominal cavity.
C, Selective posterior superior pancreaticoduodenal arteriogram after embolization with coil (*arrow*) shows no visualized aneurysm or bleeding.

low-up range, 21 months to 34 months; mean, 27.5 months), and their liver function tests were within the normal range.

Discussion

Pancreaticoduodenal artery aneurysms are uncommon but clinically important forms of vascular disease. Slightly more than 100 cases have been reported in the English-language literature. Most of these are isolated case reports. There have been only a few small series. Management of pancreaticoduodenal artery aneurysms in these reports has varied from surgery to transcatheter arterial embolization to no treatment. In our series, we performed transcatheter arterial embolization in all 10 patients. The purpose of this series was to determine which treatment for these aneurysms should be chosen in various cases.

Some researchers have reported that transcatheter arterial embolization is effective in

the treatment of visceral aneurysms, has few complications, and results in low recurrence rates [3–4, 6–9]. Coll et al. [3] reported that, since 1980, the mortality rate associated with surgery has been 19%, whereas that associated with transcatheter arterial embolization has been 0%; they reported no significant difference in the risk of recurrent hemorrhage, with rates between 0% and 5%. Despite these results, surgery is still considered by many physicians to be the initial and only definitive treatment of aneurysms involving the pancreaticoduodenal artery.

There are three major reasons for this treatment path. One is that embolization is not always technically feasible because of the difficulty of selective catheterization of the vessel feeding the aneurysm [10–14]. The second is that embolization may be associated with aneurysmal rupture during the procedure [11–12, 15]. The third is that, in the case of celiac axis stenosis or occlusion in which pancreaticoduodenal artery aneurysms are observed, transcatheter arterial embolization without bypass may lead to recurrence of pancreaticoduodenal artery aneurysm or ischemic injury as a result of the absence of major collateral vessels—that is, embolization without bypassing may be ill advised [11–12, 14, 16–19].

Catheterization of the vessels requires a proficient interventional technique; however, the advent of newer coaxial catheterization techniques has greatly improved the embolization of small, tortuous vessels. Therefore, we obtained complete embolization of all pancreaticoduodenal artery aneurysms except one, and we managed to stop the bleeding in all ruptured aneurysms. In contrast, the detection of pancreaticoduodenal artery aneurysms during surgery may fail in approximately 70% of cases [12, 20] because of their localization behind or within the parenchyma of the pancreas. Surgery may be questionable because arterial ligation (with or without aneurysm resection) is not always feasible, and partial pancreatectomy can be necessary [17–19]. In one patient in whom we tried to perform transcatheter arterial embolization 12 years ago, we could not even pack the aneurysm (i.e., we embolized only the afferent artery with microcoils). Use of the current, new coaxial catheter system or *N*-butyl cyanoacrylate injection technique [21] might be considered if we were able to do packing of or isolate the pancreaticoduodenal artery aneurysm.

In 1979, Lina et al. [15] reported aneurysm rupture secondary to transcatheter embolization. However, they did not have a coaxial catheter system at that time. To our knowledge, there have been no reports of pancreaticoduodenal aneurysm rupture secondary to transcatheter embolization since the development of the coaxial catheter system. Therefore, aneurysm rupture during the procedure should be excluded as a disadvantage of transcatheter arterial embolization.

Pancreaticoduodenal artery aneurysms can be differentiated into true and false aneurysms; the latter result from pancreatitis, abdominal trauma, surgery, or septic emboli. They often rupture into the gastrointestinal tract, whereas true aneurysms are frequently associated with stenosis or occlusion of the celiac axis and rupture into the retroperitoneal space. In patients with false pancreaticoduodenal artery aneurysms, transcatheter arterial embolization preserves vascularization of the celiac territory because false aneurysms are not usually associated with celiac artery stenosis. With regard to the third disadvantage of transcatheter arterial embolization, the controversy remains whether transcatheter arterial embolization should be done in patients with celiac artery stenosis or occlusion because transcatheter arterial embolization in vessels without major collaterals should have a higher recurrence of pancreaticoduodenal artery aneurysm or ischemic injury. Sutton and Lawton [22] postulated that stenosis of the celiac axis resulting in an increased flow through the pancreaticoduodenal artery favors the development of pancreaticoduodenal artery aneurysms. Some surgeons emphasize that the basic treatment is revascularization of the celiac trunk stenosis or occlusion [11–12, 16–19]. Two patients with celiac trunk stenosis in our series, however, had a good course without ischemic dysfunction of the liver, spleen, or duodenum, and also no recurrence of pancreaticoduodenal artery aneurysm. Some patients in other reports have had good courses without ischemic dysfunction of the liver, spleen, or duodenum [23–26]. Savastano et al. [23] reported that, although they performed embolization of pancreaticoduodenal artery aneurysms in two patients with celiac trunk stenosis and occlusion caused by compression of the median arcuate ligament, there was no recurrence of aneurysm seen at follow-ups of more than 3 years. To our knowledge, there have been no reports of the recurrence of pancreaticoduodenal artery aneurysm caused by celiac trunk stenosis or occlusion after embolization [23–27].

With regard to embolization technique of pancreaticoduodenal artery aneurysms, the best embolization technique is thought to be isolation with coils, *N*-butyl cyanoacrylate, or both, regardless of true or pseudoaneurysms. However, isolation may be absolutely impossible in half of cases. The second feasible technique, especially in the cases with pseudoaneurysm, may be embolization of the afferent artery after packing of the aneurysm. Though our sample size of the patient population was small, we have no cases in which the second feasible method resulted in failure. If a microcatheter cannot be advanced close to the aneurysm, transcatheter arterial embolization may be an insufficient method regardless of decreasing blood flow. In such a case, direct percutaneous embolization technique can be useful in selected patients. In this method, *N*-butyl cyanoacrylate, not coils, should be used as embolization materials.

Preoperative angiography has played an important role in facilitating surgical management [12]. Coil embolization is useful to decrease blood flow and to temporarily stop bleeding, even if embolization of the efferent artery cannot be achieved. The less-invasive transcatheter arterial embolization, by which diagnosis and treatment can be performed simultaneously, should be performed as an initial treatment.

In conclusion, transcatheter arterial embolization should be an initial treatment for ruptured or unruptured pancreaticoduodenal artery aneurysms regardless of whether surgery needs to be performed, and it is an initial safe and effective method of therapy in both elective and emergency cases.

References

1. Stabile BE, Wilson SE, Debas HT. Reduced mortality from bleeding pseudocysts and pseudoaneurysms caused by pancreatitis. *Arch Surg* 1983; 118:45–51
2. Iyomasa S, Matsuzaki Y, Hiei K, et al. Pancreaticoduodenal artery aneurysm: a case report and review of the literature. *J Vasc Surg* 1995; 22:161–166
3. Coll DP, Ierardi R, Kerstein MD, et al. Aneurysms of the pancreaticoduodenal arteries: a change in management. *Ann Vasc Surg* 1998; 12:286–291
4. Mandel SR, Jaques PF, Mauro MA, et al. Nonoperative management of peripancreatic arterial aneurysms: a 10-year experience. *Ann Surg* 1987; 205:126–128
5. Drooz AT, Lewis CA, Allen TE, et al. Quality improvement guidelines for percutaneous transcatheter embolization. SCVIR Standards of Practice Committee. Society of Cardiovascular & Interventional Radiology. *J Vasc Interv Radiol* 1997; 8:889–895

6. Carr SC, Pearce WH, Vogelzang RL, et al. Current management of visceral artery aneurysms. *Surgery* 1996; 120:627–634
7. Yoneyama F, Tsuchie K, Kuno T, et al. Aneurysmal rupture of the pancreaticoduodenal artery successfully treated by transcatheter arterial embolization. *J Hepatobiliary Pancreat Surg* 1998; 5:104–107
8. Jeroudi AA, Belli AM, Shorvon PJ. False aneurysm of the pancreaticoduodenal artery complicating therapeutic endoscopic retrograde cholangiopancreatography. *Br J Radiol* 2001; 74:375–377
9. Itoh K, Kamiya Y, Ohno N, et al. A case of pancreaticoduodenal artery aneurysm causing pancreatic pseudotumor and duodenal obstruction. *Eur J Gastroenterol Hepatol* 2002; 14:457–461
10. Chiang KS, Johnson CM, McKusick MA, et al. Management of inferior pancreaticoduodenal artery aneurysms: a 4-year, single center experience. *Cardiovasc Intervent Radiol* 1994; 17:217–221
11. Neschis DG, Safford SD, Golden MA. Management of pancreaticoduodenal artery aneurysms presenting as catastrophic intraabdominal bleeding. *Surgery* 1998; 123:8–12
12. de Perrot M, Berney T, Deleaval J, et al. Management of true aneurysms of the pancreaticoduodenal arteries. *Ann Surg* 1999; 229:416–420
13. Carmeci C, McClenathan J. Visceral artery aneurysms as seen in a community hospital. *Am J Surg* 2000; 179:486–489
14. Watanabe A, Kunieda K, Saji S. A ruptured pancreaticoduodenal artery aneurysm associated with a splenic artery aneurysm: report of a case. *Surg Today* 2001; 31:542–545
15. Lina JR, Jaques P, Mandell V. Aneurysm rupture secondary to transcatheter embolization. *AJR* 1979; 132:553–556
16. Stanley JC, Wakefield TW, Graham LM, et al. Clinical importance and management of splanchnic artery aneurysms. *J Vasc Surg* 1986; 3:836–840
17. Kabaroudis A, Papaziogas B, Papaziogas T. Spontaneous retroperitoneal hematoma caused by aneurysm of the inferior pancreaticoduodenal artery. *Am J Surg* 2002; 184:174–175
18. Taylor AJN, Hershman MJ, Hadjiminar D, et al. Pancreaticoduodenal artery aneurysm: diagnostic and management difficulties. *J R Soc Med* 1993; 86:356–357
19. Paty PSK, Cordero JA Jr., Clement Darling R, et al. Aneurysms of the pancreaticoduodenal artery. *J Vasc Surg* 1996; 23:710–713
20. Retzlaff JA, Hagedorn AB, Bartholomew LG. Abdominal exploration for gastrointestinal bleeding of obscure origin. *JAMA* 1961; 177:104
21. Yamakado K, Nakatsuka A, Tanaka N, et al. Transcatheter arterial embolization of ruptured pseudoaneurysms with coils and n-butyl cyanoacrylate. *J Vasc Interv Radiol* 2000; 11:66–72
22. Sutton D, Lawton G. Coeliac stenosis or occlusion with aneurysm of the collateral supply. *Clin Radiol* 1973; 24:49–53
23. Savastano S, Feltrin GP, Miotto D, et al. Embolization of ruptured aneurysm of the pancreaticoduodenal artery secondary to long-standing stenosis of the celiac axis. *Vasc Surg* 1995; 29:309–314
24. Uher P, Nyman U, Ivancev K, et al. Aneurysm of the pancreaticoduodenal artery associated with occlusion of the celiac artery. *Abdom Imaging* 1995; 20:470–473
25. Kobayashi S, Yamaguchi A, Isogai M, et al. Successful transcatheter embolization of a pancreaticoduodenal artery aneurysm in association with celiac axis occlusion: a case report. *Hepato-Gastroenterology* 1999; 46:2991–2994
26. Ogino H, Sato Y, Banno T, et al. Embolization in a patient with ruptured anterior inferior pancreaticoduodenal arterial aneurysm with median arcuate ligament syndrome. *Cardiovasc Intervent Radiol* 2002; 25:318–319
27. Arao T, Ishida E, Nishina S, et al. Catastrophic intraabdominal bleeding due to rupture of pancreaticoduodenal artery aneurysm: successful transcatheter arterial embolization. *Pancreas* 2003; 26:99–100

PO Box 2345, Beijing 100023, China
www.wjgnet.com
wjg@wjgnet.com

World J Gastroenterol 2006 July 14; 12(26): 4214-4218
World Journal of Gastroenterology ISSN 1007-9327
© 2006 The WJG Press. All rights reserved.

RAPID COMMUNICATION

Liver microcirculation after hepatic artery embolization with degradable starch microspheres *in vivo*

Jian Wang, Satoru Murata, Tatsuo Kumazaki

Jian Wang, Department of Interventional Radiology and Vascular Surgery, The First Hospital of Peking University, 100034, Beijing, China
Satoru Murata, Tatsuo Kumazaki, Department of Radiology, Nippon Medical School, Tokyo, Japan
Correspondence to: Jian Wang, Department of Interventional Radiology and Vascular Surgery, the First Hospital of Peking University, 100034, Beijing, China. vanjian@sohu.com
Telephone: +86-10-66518436 Fax: +86-10-66518436
Received: 2005-11-12 Accepted: 2005-12-07

Abstract

AIM: To observe the dynamic changes of liver microcirculation *in vivo* after arterial embolization with degradable starch microspheres (DSM).

METHODS: DSM were injected into the proper hepatic artery through a silastic tube inserted retrogradely in gastroduodenal artery (GDA) of SD rats. Fluorescent microscopy was used to evaluate the dynamic changes of blood flow through the terminal portal venules (TPVs), sinusoids and terminal hepatic venules (THVs). The movements of DSM debris were also recorded. Six hours after injection of DSM, percentages of THVs with completely stagnant blood flow were recorded.

RESULTS: Two phases of blood flow change were recorded. In phase one: after intra-arterial injection of DSM, slow or stagnant blood flow was immediately recorded in TPVs, sinusoids and THVs. This change was reversible, and blood flow resumed completely. In phase two: after phase one, blood flow in TPVs changed again and three patterns of blood flow were recorded. Six hours after DSM injection, 36.9% ± 9.2% of THVs were found with completely stagnant blood flow.

CONCLUSION: DSM can stop the microcirculatory blood flow in some areas of liver parenchyma. Liver parenchyma supplied by arteries with larger A-P shunt is considered at a higher risk of total microcirculatory blood stagnation after injection of DSM through hepatic artery.

© 2006 The WJG Press. All rights reserved.

Key words: Degradable starch microsphere; Hepatic microcirculation; Hepatic arteries; Fluorescence; Transarterial chemoembolization

Wang J, Murata S, Kumazaki T. Liver microcirculation after hepatic artery embolization with degradable starch microspheres *in vivo*. *World J Gastroenterol* 2006; 12(26): 4214-4218

http://www.wjgnet.com/1007-9327/12/4214.asp

INTRODUCTION

It has been accepted that transarterial chemoembolization (TACE) is an effective method to treat the unresectable hepatocellular carcinoma (HCC). With the characteristics of long retention time in the tumor tissue, iodinated poppyseed oil (Lipiodol) has been frequently used as the embolization material in clinical practice[1-4]. Animal experiments demonstrated that after injection of iodized oil into the hepatic artery, small Lipiodol drops could be found in the terminal portal venules (TPVs), which was assumed passing through the pathway of arterial-portal anastomosis such as the peribiliary pluxes[5-7]. When Lipiodol drops flow into the sinusoids, they can severely occlude the blood flow, cause the stagnation of local microcirculation, and further lead to ischemic liver parenchyma injury[8,9]. Super-selective technique with microcatheter and guidewires has been considered as a safe and effective way to treat HCC. Under some conditions in which liver function is severely damaged or blood supply of HCC is so complex that it is impossible to super-select the tumor feeding arteries, TACE is developed. Degradable starch microspheres (DSM), a temporary artery embolizer has been increasingly used as an alternative to Lipiodol in some particular situations[10-12]. It has also been suggested that, when the tumor feeding artery cannot be super-selected by microcatheter and guidewire, one-shot injection of DSM before TACE can be regarded as a practical method to protect the tumor free liver tissue from the injury caused by Lipiodol inflow following TAE. To fully understand its effects on liver microcirculation, we injected DSM through proper hepatic artery of rats, and the dynamic changes of liver microcirculation were evaluated by *in vivo* fluorescent microscopic observations.

MATERIALS AND METHODS

Animal model

Ten Sprague-Dawley rats weighing 300 to 450 g were used in compliance with the regulations and the Guide for the Care and Use of Laboratory Animals. The animals were

Table 1 Blood flow stagnation time and recovery time

No.	Start of blood flow stagnation	Time of complete recovery of blood flow
1	1.1	10.9
2	1.4	13.1
3	2.6	15
4	1	14.9
5	1.6	9.82
6	2.3	11.5
7	2.8	13.2
8	3	14.5
9	2.8	14.3
10	1.6	9.47
mean ± SD	2.0 ± 0.8	12.7 ± 2.1

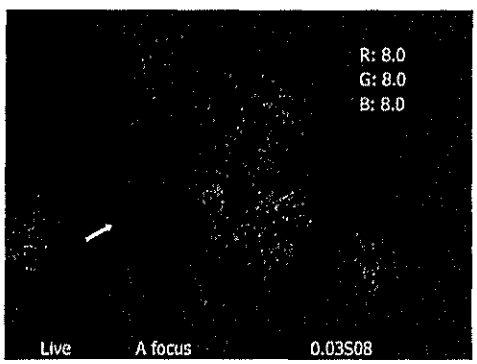

Figure 1 Normal microcirculation of the rat liver. Arrow: TPV, Opened arrow: THV.

fed with standard food pellets and tap water *ad libitum*. They were deprived of food but obtained free access to water for 12 h before the experiments. Anesthesia was performed by intra-peritoneal injection of 50 mg/kg sodium pentobarbital. The left femoral vein was cannulated with a 1F silastic tube (Natsume Corp. Tokyo, Japan) for additional anesthesia and liquid transfusion during the procedure. After a midline abdominal incision, the liver was carefully retracted to expose the gastroduodenal artery (GDA), which was catheterized by another 1F silastic tube (Natsume Corp., Tokyo, Japan) with its tip placed before the bifurcation that leads to the proper hepatic artery. The left lobe of liver was gently exteriorized and positioned over the window of the microscope stage. The liver parenchyma was covered with a small piece of plastic wrap; its surface was constantly irrigated with Ringer's solution at the body temperature.

Fluorescence microscopy

The exteriorized left liver lobe was transilluminated with monochromatic light generated by a prism monochromator equipped with a xenon lamp. Microscopic images of the microvasculatures were obtained with objective lenses (magnification, × 10, × 20) and an ocular lens (magnification, × 10). DSM (Yakult Honsha Co., Ltd., Tokyo, Japan) 12 mg in 0.2 mL was prepared in a 1 mL syringe and the solution was made uniform before injection. After infusion of 1 g/L fluorescent sodium 0.1 mL into the cannulated GDA, DSM was injected gently in one minute. The *in vivo* microscopic images of the following procedure were recorded on videotapes.

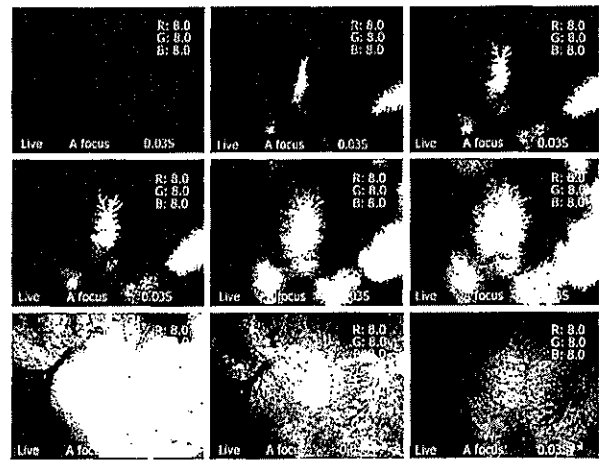

Figure 2 After infusion of fluorescent sodium from the GDA to proper hepatic artery, blood flow from TPVs to THVs through sinusoids can be clearly visualized.

In vivo evaluation

For each rat, areas with best visualization were selected for evaluation. Six hours later, 1 g/L fluorescent sodium 0.1 mL was infused through the cannulated left femoral vein to check the whole surface of liver lobe for a complete confirmation of the liver microcirculation. One hundred THVs were randomly selected during the horizontal and vertical movements of the microscope. THVs with completely stopped blood flow were statistically counted.

Statistical analysis

Data analysis was performed employing the Statistical Package for the Social Sciences Version 12.0 for Windows (SPSS® Inc., Chicago IL, USA). Results of the descriptive statistical analysis were presented as mean ± SD.

RESULTS

Clear images of the liver microcirculation (TPVs, sinusoids, and THVs) could be seen under *in vivo* fluorescent microscope (Figure 1). Blood flow from one TPV was drained through the sinusoids into several THVs; similarly, one particular THV provided venular drainage for several TPVs. Hepatic arterioles, the other afferent vessels in the liver, usually could not be visualized (Figure 2).

Blood flow in TPVs after DSM injection

Blood flow through TPVs demonstrated an immediate response after DSM injection. The speed of blood flow dropped dramatically at once. In 2.0 ± 0.8 min (Max 3 min), the blood flow in the observed area completely stopped. After that, blood flow through TPVs resumed gradually; 12.7 ± 2.1 min (Max 15 min) after injection of the DSM, blood flow through TPVs completely recovered (Table 1). No evidence of DSM or its disaggregated debris could be recorded within this time interval. For convenient explanation, we named this period as "phase one", and the

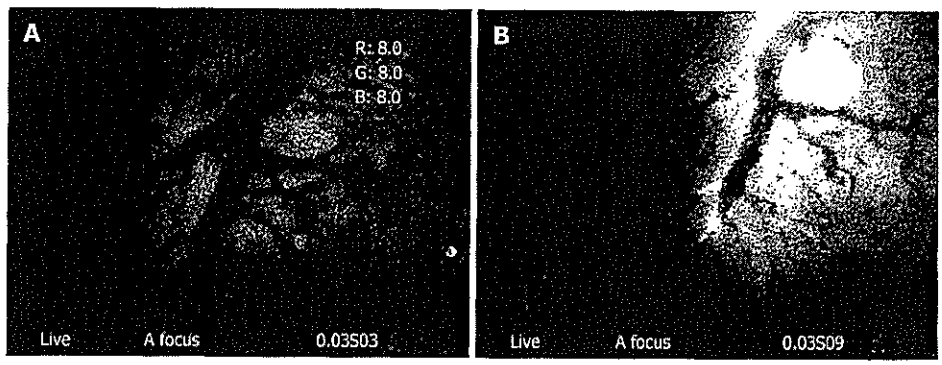

Figure 3 A: Small debris can enter sinusoids through TPV (arrow); B: The same TPV as image 3, debris of DSM continuously enter sinusoids through TPV, blood flow in TPV is intermittent but not stagnant.

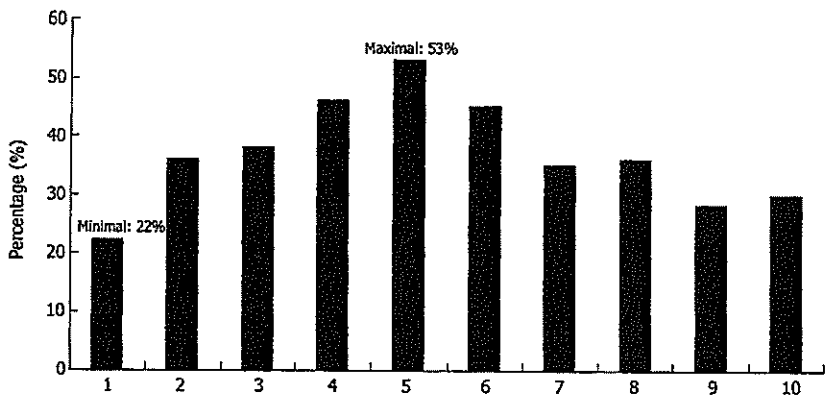

Figure 4 Percentage of the completely stagnant THVs 6 h after DSM injection in 10 rats. The minimal percentage is 22%, and the maximal is 53%.

blood flow changes afterward as "phase two". In phase two, three different types of blood flow changes in TPVs could be recorded.

Type one: The speed of blood flow slowed down again, and then completely stopped. This phenomenon could be found as early as 25 min after DSM injection and last for the whole procedure. The TPVs could never resume their blood flow during the observational period. DSM or its debris could be hardly found in TPVs in this type.

Type two: The speed of blood flow in TPVs decreased at different level, either slightly striking or some times intermittent, however the stagnation was not recorded during the whole observation time. Numerous small pieces of debris with irregular shapes could be found to flow through and drain into the distal sinusoids (Figure 3A and B).

Type three: In particular areas, TPVs kept a constant flow after phase one. The blood flow did not change during the whole procedure. DSM or its debris could not be recorded in these TPVs.

Blood flow in sinusoids and THVs

The blood flow through sinusoids and THVs followed the changes of TPVs in phase one. They also demonstrated a dramatic decrease of blood flow speed after DSM injection. Some even completely stopped. Nevertheless, it could be fully recovered.

During the following period, three kinds of blood flow, similar to that of the TPVs could also be recorded in sinusoids and THVs, ie, completely stagnant blood flow, intermittent and slow flow, normal flow.

DSM debris in the hepatic microvasculature

Twenty minutes (the earliest time) after injection of DSM, small pieces of debris could be found in some sinusoids. Some of the debris, with a relatively small size, could directly pass through the sinusoids and flow into THVs. Some debris, with larger size, could occlude the corresponding sinusoids. This occlusion was temporary; recanalization could be achieved by opening of collaterals or further distal movement of the disaggregated debris. The number of DSM debris reached a peak value 1 h after DSM injection. No DSM particles with the original size and shape could be found in sinusoids and THVs. Numerous disaggregated debris with small diameter entered the THVs.

Hepatic microcirculation after DSM injection

Six hours after DSM injection, the brightness of the liver surface was not uniform after infusion of fluorescent sodium through the femoral vein, suggesting the heterogeneous nature of the liver blood flow. Areas with completely stagnant blood flow in TPVs, THVs and sinusoids could be found sparsely distributed among the areas with normal or sluggish blood flow. Approximately 36.9% ± 9.2% of randomly selected THVs were found with completely stagnant blood flow (Figure 4).

DISCUSSION

DSM is a kind of embolization material that can temporarily occlude the vessels. The degradation of

DSM is considered to be caused by a combination of the chemical effects of amylase and the striking force of the vortexial arterial flow. Hepatic arterial perfusion is essential for an optimal sinusoidal function because it maintains transinusoidal pressure[13]. After intra-artery injection of DSM, immediately slow down or even stop of the blood flow in TPVs, sinusoids, and THVs could be found. It is considered that a sudden reduction of arterial blood flow is caused by numerous DSM casts embolization. The blocked blood flow could soon be resumed due to a compensatory increase of portal blood flow as a buffer response. This can explain the phenomenon of phase one which happened after the DSM injection. After a complete recovery of blood flow in phase one, presinusoidal A-P shunt[14-16] should be the reason for the appearance of three types of blood flow in phase two. We have found in our previous study that after intra-arterial injection of DSM, various sizes of DSM casts are formed inside the arterioles which can block the arterial blood flow. The proximal end of DSM casts will disaggregate under the pumping force of vortexial arterial blood flow. Debris with different sizes will be discharged at the proximal end and further occlude the branch of the original artery. We presume that A-P shunts have various size, some larger debris of the disaggregated DSM can pass through larger A-P shunts and reach the portal side that is proximal to TPVs. Debris accumulated at the portal side form a number of emboli. These emboli, if big enough, will completely shut the portal blood flow to distal TPVs and be harder to disaggregate because the pumping force of portal blood stream is much weaker than that of the arterial one. This means, at certain areas of liver parenchyma, both arterial and portal blood flows are stopped by DSM casts and the debris emboli. Few debris could be found in the distal TPVs because the proximal portion of TPVs was completely occluded by the debris emboli. This explains the type one phenomenon. For some small A-P shunt, only small-sized debris can pass through; and these smaller debris could partially occlude portal branch and was easily to be pushed distally. Some could reach TPVs and flow through sinusoids to THVs. This caused type two phenomenon. As for the type three phenomenon, it is considered that no debris of DSM entered portal site through A-P shunt.

After entering sinusoids, debris could occlude sinusoids. For a single sinusoid, the blood flow can be resumed either by further disaggregation of the debris or by opening of the small collaterals. Small DSM debris, when passing through sinusoid, will flow freely into THVs. Six hours after injection of DSM, we found 22%-53% (mean: 36.9% ± 9.2%) of THVs with totally stagnant blood flow. That means all sinusoids draining blood to these THVs had been stagnant in blood flow. The corresponding liver parenchyma received no fresh blood supply during this time. The cause of stagnant blood flow in sinusoids surrounding THVs is presumed at the presinusoidal level. We assume that the occlusion site was the presinusoidal portal vein with relatively larger diameter. After arterial embolization by DSM casts, the more bigger debris of DSM entered this portion through larger A-P shunt and accumulation of these debris formed intravascular emboli. Weak pumping force of portal blood flow could not disaggregate these emboli, and the amylase could take effects more slowly because little fresh blood flow could reach those emboli. With all those factors, the emboli could maintain stable during a fairly long period of time. Thus, a simultaneous blockade of the arterial and portal blood flow could lead to a completely stagnant blood flow in distal sinusoids. Because the amylase in blood flow will chemically disaggregate the DSM and its debris, whether the TPVs, sinusoids and THVs can resume their blood flow later needs to be further studied.

It is preliminarily confirmed in this study that DSM, with its degradation products, can enter portal vein through hepatic arterial injection. It can completely stop the microcirculatory blood flow in some areas of liver parenchyma. A-P shunt is considered to be a determining factor during the procedure. Liver parenchyma supplied by arteries with larger A-P shunt is presumed to have higher risk of total microcirculatory blood stagnation after injection of DSM through hepatic artery. Whether the use of DSM can provide protective effects during TACE awaits further evaluation.

REFERENCES

1 Kim P, Prapong W, Sze DY, So SK, Razavi MK. Treatment of hepatocellular carcinoma with sub-selective transcatheter arterial oily chemoinfusion. *Tech Vasc Interv Radiol* 2002; 5: 127-131

2 Lo CM, Ngan H, Tso WK, Liu CL, Lam CM, Poon RT, Fan ST, Wong J. Randomized controlled trial of transarterial lipiodol chemoembolization for unresectable hepatocellular carcinoma. *Hepatology* 2002; 35: 1164-1171

3 Chen MS, Li JQ, Zhang YQ, Lu LX, Zhang WZ, Yuan YF, Guo YP, Lin XJ, Li GH. High-dose iodized oil transcatheter arterial chemoembolization for patients with large hepatocellular carcinoma. *World J Gastroenterol* 2002; 8: 74-78

4 Bhattacharya S, Dusheiko GM. Treatment of unresectable hepatocellular carcinoma: targeted therapies using iodized oil. *Princess Takamatsu Symp* 1995; 25: 253-264

5 Kan Z, Sato M, Ivancev K, Uchida B, Hedgpeth P, Lunderquist A, Rosch J, Yamada R. Distribution and effect of iodized poppyseed oil in the liver after hepatic artery embolization: experimental study in several animal species. *Radiology* 1993; 186: 861-866

6 Kan Z, Wallace S. Sinusoidal embolization: impact of iodized oil on hepatic microcirculation. *J Vasc Interv Radiol* 1994; 5: 881-886

7 Kan Z, Ivancev K, Hagerstrand I, Chuang VP, Lunderquist A. In vivo microscopy of the liver after injection of Lipiodol into the hepatic artery and portal vein in the rat. *Acta Radiol* 1989; 30: 419-425

8 Akashi Y, Koreeda C, Mizuno T, Inoue K, Kawa SK, Tanaka Y. Hepatic parenchymal changes after the intraarterial injection of lipiodol in tumor-bearing rabbits. *Invest Radiol* 1993; 28: 128-132

9 Sato M, Yamada R, Uchida B, Hedgepeth P, Rosch J. Effects of hepatic artery embolization with Lipiodol and gelatin sponge particles on normal swine liver. *Cardiovasc Intervent Radiol* 1993; 16: 348-354

10 Furuse J, Ishii H, Satake M, Onaya H, Nose H, Mikami S, Sakai H, Mera K, Maru Y, Yoshino M. Pilot study of transcatheter arterial chemoembolization with degradable starch microspheres in patients with hepatocellular carcinoma. *Am J Clin Oncol* 2003; 26: 159-164

11 Kigami Y, Kobayashi H, Umeoka S, Emoto T, Akuta K. Early effect of intra-arterial chemotherapy combined with degradable starch microspheres for malignant hepatic tumors.

Gan To Kagaku Ryoho 2003; 30: 81-87
12 **Katsumata K**, Tomioka H, Sumi T, Yamasaki T, Takagi M, Kato F, Suzuki Y, Aoki T, Koyanagi Y. Liver metastasis of pancreatic cancer managed by intra-arterial infusion chemotherapy combined with degradable starch microspheres. *Int J Clin Oncol* 2003; 8: 110-112
13 **Alexander B**, Cottam H, Naftalin R. Hepatic arterial perfusion regulates portal venous flow between hepatic sinusoids and intrahepatic shunts in the normal rat liver in vitro. *Pflugers Arch* 2001; 443: 257-264
14 **Grisham JW**, Nopanitaya W. Scanning electron microscopy of casts of hepatic microvessels: review of methods and results. In: Lautt WW (ed) Hepatic circulation in health and disease. New York: Raven Press, 1981: 87-109
15 **McCuskey RS**. A dynamic and static study of hepatic arterioles and hepatic sphincters. *Am J Anat* 1966; 119: 455-477
16 **Bookstein JJ**, Cho KJ, Davis GB, Dail D. Arterioportal communications: observations and hypotheses concerning transsinusoidal and transvasal types. *Radiology* 1982; 142: 581-590

S- Editor Pan BR L- Editor Zhu LH E- Editor Bi L

CardioVascular and Interventional Radiology

© Springer Science+Business Media, Inc. 2005
Published Online: 21 June 2005

Cardiovasc Intervent Radiol (2006) 29:155–156
DOI: 10.1007/s00270-003-0172-0

Pulmonary Artery Perforation Repair During Thrombectomy Using Microcoil Embolization

Hiroyuki Tajima, Satoru Murata, Tatsuo Kumazaki, Yutaka Abe, Teruo Takano

Department of Radiology/Center for Advanced Medical Technology, and Department of Internal Medicine I, Nippon Medical School, 1-1-5, Sendagi, Bunkyo-ku, Tokyo 113-8602, Japan

Abstract

A distal pulmonary artery perforation was successfully occluded by percutaneous microcoil embolization via a microcatheter. Microcoil embolization is a reasonable alternative therapeutic approach for this rare complication of pulmonary interventional procedures.

Key words: Catheters and catheterization—Embolism, pulmonary—Interventional procedure, complications—Perforation—Pulmonary artery

Pulmonary artery (PA) perforation is a rare but serious complication of percutaneous pulmonary intervention. We describe a case of PA perforation treated successfully by microcoil embolization.

Case Report

A 78-year-old woman with sudden onset of hypotensive shock was transferred to the coronary care unit, receiving mechanical ventilation, intra-aortic balloon pumping, and positive inotropic support with high-dose catecholamines. Baseline cineangiography depicted total occlusion of segment 4 AV (postero-lateral artery, American Heart Association Classification), which failed catheter intervention. Swan-Ganz catheterization revealed pulmonary hypertension (56/21(31) mmHg), which raised the suspicion of pulmonary thromboembolism.

Pulmonary angiography was performed the next day using a combination of digital subtraction angiography and a rotational digital angiography system [1], and showed bilateral massive pulmonary thromboembolism. The groin hematoma due to the initial high-dose heparin administration was very severe. Thrombolytic therapy was contraindicated; manual thromboaspiration was planned [2, 3]. Approval for this procedure was obtained from the local university ethics committee, and written informed consent was obtained from the patient.

First, an 8 Fr long sheath complete with a hemostatic valve (Medi-kit, Japan) is placed in the main PA. Then, the PTCA guiding catheter (8 Fr Guider RJ-5, Cordis, USA) is advanced into the thrombus. A 10 ml syringe with a luer lock connector is used to apply suction while the catheter is moved slowly to and fro over several centimeters within the PA. If blood readily enters the syringe, the clot has cleared the catheter. The syringe is then removed and its contents are expressed over a gauze-draped basin.

Multiple aspirations were performed, and a large amount of thrombus was aspirated. Slightly bloody sputum was aspirated from the endotracheal tube during the procedure. The patient remained hemodynamically stable. Confirmative pulmonary angiography revealed contrast material leaking from the midportion of the left lower-posterior branch (segment 10 artery, A-10) (Fig. 1). A 2.3 Fr Rapid-Transit infusion catheter (Cordis Neurovascular, FL, USA) was introduced over the guidewire (Transend-Ex, 0.014 inch, Boston Scientific Target, CA, USA) in the midportion of A-10. Through the microcatheter, a 0.018-inch platinum coil (Tornade, Cook, IN, USA) was advanced using a guidewire. Five coils (two tapered 2 mm to 5 mm; three tapered 2 mm to 4 mm) were placed in the left A-10 just proximal to the perforation site. Repeat pulmonary angiography demonstrated occlusion of the injured artery with no evidence of extravasation of contrast material (Fig. 2). The embolization procedure took 14 min.

The patient remained hemodynamically stable, and received heparin/urokinase therapy gradually in the coronary care unit. Repeat pulmonary angiography 7 days after the procedure showed no perforation and excellent recovery of the pulmonary circulation. The patient's postoperative course was uneventful, and she went to the general ward 14 days after admission.

Discussion

Acute massive pulmonary thromboembolism is a severe condition creating hemodynamic instability that has been shown to have a mortality rate of more than 30%. Rapid recovery of pulmonary flow is essential for preventing mortality, and simultaneously causes significant hemodynamic improvement. Intravenous administration of thrombolytic agents is the mainstay of therapeutic management in such cases [4]. When thrombolytic therapy fails or is contraindicated, percutaneous catheter treatment may represent an additional option [5].

Percutaneous aspiration thrombectomy has evolved from a very simple concept that has been used previously in many fields [6–8]. The use of a large-lumen PTCA guiding catheter for pulmonary clot aspiration has been reported [2, 3]. The advantages of this technique are that it is less invasive for the vessels, it is convenient (because it uses an 8 Fr, small introducer sheath and a conventional PTCA guiding catheter it may be performed in a standard angiography laboratory), and it incurs a low cost.

Pulmonary artery perforation associated with this procedure has not yet been reported. Tight connection of the organized thrombus to the native arterial wall and rough catheter management must be the leading cause of the perforation in this case.

Coronary artery perforation is a relatively uncommon but morbid complication of percutaneous coronary intervention. Percutaneous embolizations with microcoils, gelfoam, polyvinyl alcohol, autogenous clots, and thrombin are reported with high success [9–13]. We selected microcoils because of their daily usage in our department.

Correspondence to: Hiroyuki Tajima; *email:* h-tajima@nms.ac.jp

Fig. 1. Pulmonary angiography demonstrating extravasation of contrast (arrow).

Fig. 2. Angiography demonstrating successful treatment of pulmonary artery perforation. The left lower posterior branch is occluded with microcoils (arrow), and contrast extravasation is no longer visible.

In conclusion, microcoil embolization provides a rapid and safe method of sealing PA perforation. The method appears to be especially useful in high-risk patients, and is a minimally invasive alternative to surgical therapy.

Acknowledgment. This work was supported in part by a research Project Grant-in Aid for Scientific Research (C2) (Project number 12670907) from the Ministry of Education, Culture, Sports, Science and Technology, Japan.

References

1. Tajima H, Kumazaki T, Kawamata H, Ichikawa K, Takano T (2001) Development of rotational digital angiography system: Clinical value in acute pulmonary thromboembolism. Comput Methods Programs Biomed 66:111–114
2. Hiramatsu S, Ogihara A, Kitano Y, Mashiko M, Iseki S, Muramatsu J, Izumi T (1999) Clinical outcome of catheter fragmentation and aspiration therapy in patients with acute pulmonary embolism. J Cardiol 34:71–78 (abstract in English)
3. Takashina A, Inoue I, Inoue T, Sakai K (1996) Embolectomy by catheter for acute pulmonary thromboembolism. J Jpn Coll Angiol 36:387–394 (abstract in English)
4. Stock KW, Jacob AL, Schnabel KJ, Bengartz G, Steinbrich W (1997) Massive pulmonary embolism: Treatment with thrombus fragmentation and local fibrinolysis with recombinant human-tissue plasminogen activator. Cardiovasc Intervent Radiol 20:364–368
5. Uflacker R (2001) Intervention therapy for pulmonary embolism. J Vasc Interv Radiol 12:147–164
6. Starck EE, McDermott JC, Crummy AB, Turnipseed WD, Acher CW, Burgess JH (1985) Percutaneous aspiration thrombectomy. Radiology 156:61–66
7. Morgan R, Belli AM (2002) Percutaneous thrombectomy: a review. Eur Radiol 12:205–217
8. Turmel-Rodrigues L, Sapoval M, Pengloan J, et al. (1997) Manual thromboaspiration and dilation of thrombosed dialysis access: Midterm results of a simple concept. J Vasc Interv Radiol 8:813–824
9. Ajluni SC, Grazier S, Blankenship L, O'Neill WW, Safian RD (1994) Perforations after coronary interventions: Clinical, angiographic, and therapeutic observations. Cathet Cardiovasc Diagn 32:206–212
10. Gaxiola E, Browne KF (1998) Coronary artery perforation repair using microcoil embolization. Cathet Cardiovasc Diagn 43:474–476
11. Dixon SR, Webster MW, Ormiston JA, Wattie WJ, Hammett CJK (2000) Gelfoam embolization of a distal coronary artery guidewire perforation. Cathet Cardiovasc Interv 49:214–217
12. Mahmud E, Douglas Jr JS (2001) Coil embolization for successful treatment of perforation of chronically occluded proximal coronary artery. Cathet Cardiovasc Interv 53:549–552
13. Fischell TA, Korban EH, Lauer MA (2003) Successful treatment of distal coronary guidewire-induced perforation with balloon catheter delivery of intracoronary thrombin. Cathet Cardiovasc Interv 58:370–374

REIC/Dkk-3 as a potential gene therapeutic agent against human testicular cancer

RYUTA TANIMOTO[1], FERNANDO ABARZUA[1], MASAKIYO SAKAGUCHI[2], MIKIRO TAKAISHI[2], YASUTOMO NASU[1], HIROMI KUMON[1] and NAM-HO HUH[2]

Departments of [1]Urology and [2]Cell Biology, Okayama University Graduate School of Medicine, Dentistry and Pharmaceutical Sciences, Shikata-chou, Okayama 700-8558, Japan

Received June 23, 2006; Accepted August 29, 2006

Abstract. Human testicular cancer is very sensitive to chemotherapy and radiation therapy and is regarded as a curable cancer. The cancer prevails in the young reproductive generation and testicular dysfunction is often observed as a side effect, remaining a serious challenge. In the present study, we examined the potential utility of REIC/Dkk-3-based gene therapy against human testicular cancer. Expression of REIC/Dkk-3 was reduced in all of the human seminoma and non-seminomatous germ cell tumor tissues. Overexpression of REIC/Dkk-3 using an adenovirus vector (Ad-REIC) induced apoptosis in a testicular germ cell cancer cell line NCCIT but not in normal human fibroblasts. c-Jun terminal kinase (JNK) was activated by Ad-REIC and the induction of apoptosis was abrogated by a JNK inhibitor. A single intratumoral injection of Ad-REIC markedly inhibited the tumorigenic growth of NCCIT cells in nude mice. These results indicate that Ad-REIC may lead to developing less insulting and non-genotoxic therapeutic measures against human testicular cancer.

Introduction

Testicular cancer is the most common malignant disease occurring in young adult men. Although the incidence of testicular cancer in the general population is not remarkably high, it has been steadily increasing in recent decades (1). The majority of testicular cancer, i.e., 90~95%, derives from germinal cells and is broadly classified as seminoma and non-seminomatous germ cell tumors (NSGCTs) (2). Testicular germ cell cancer is known to be highly sensitive to chemotherapy and radiation therapy. The rate of complete cure for patients with germ cell cancer is higher than 90% and nearly all cases can be cured when at lower stages of tumor progression (3). Chemotherapy and radiation therapy, however, often result in unfavorable complications, including testicular dysfunction and infertility (4-6), secondary malignancies (7-9) and, less seriously, renal dysfunction and hearing disturbance (10). Oligospermia or aspermia is usually transient and many cured patients father children (11). Considering the young age of most patients, however, the forced interruption of conception attempts and possible necessity of reproductive assistance using cryo-preserved semen should not be overlooked. Less insulting and non-genotoxic therapeutic measures are certainly preferable for cancers arising in the gonadal organ.

REIC/Dkk-3 was originally isolated as a gene whose expression was reduced in immortalized human fibroblasts compared with that in normal counterparts (12), and subsequent analyses revealed that it is a candidate tumor suppressor gene (13). Expression of the REIC/Dkk-3 gene was reduced in many human cancer cells and tissues including prostate cancer, renal clear cell carcinoma, and non-small cell lung cancer (14-16). Forced expression of REIC/Dkk-3 using an adenovirus vector selectively induced apoptotic cell death in human prostate cancer cell lines with marginal effect in normal epithelial and stroma cells of prostate (16). The apoptosis involved JNK activation, mitochondrial translocation of Bax, and reduction of Bcl-2. In an animal model where human prostate cancer cells were subcutaneously transplanted in nude mice, a single injection of the adenovirus vector carrying REIC/Dkk-3 showed remarkable therapeutic effect, i.e., complete regression of the tumor in 4 of the 5 animals transplanted (16). Adenovirus vector is known to be hardly integrated into genomic DNA and thus non-genotoxic (17,18). These results indicate the possible utility of REIC/Dkk3 as a selective non-genotoxic therapeutic measure. In the present study, therefore, we examined the expression of REIC/Dkk-3 in testicular cancers and the possible therapeutic effect of the overexpression of REIC/Dkk-3 on human testicular cancer cells.

Materials and methods

Tissues, cells and reagents. A testicular carcinoma tissue microarray was purchased from Folio Biosciences (Columbus, OH). Surgically resected testicular cancer tissues were fixed with 4% paraformaldehyde and tissue sections were made under conventional conditions. NCCIT, a cell line established

Correspondence to: Dr N. Huh, Department of Cell Biology, Okayama University Graduate School of Medicine, Dentistry, and Pharmaceutical Sciences, 2-5-1 Shikata-cho, Okayama 700-8558, Japan
E-mail: namu@md.okayama-u.ac.jp

Key words: REIC, Dkk-3, testicular tumor, NCCIT, therapy

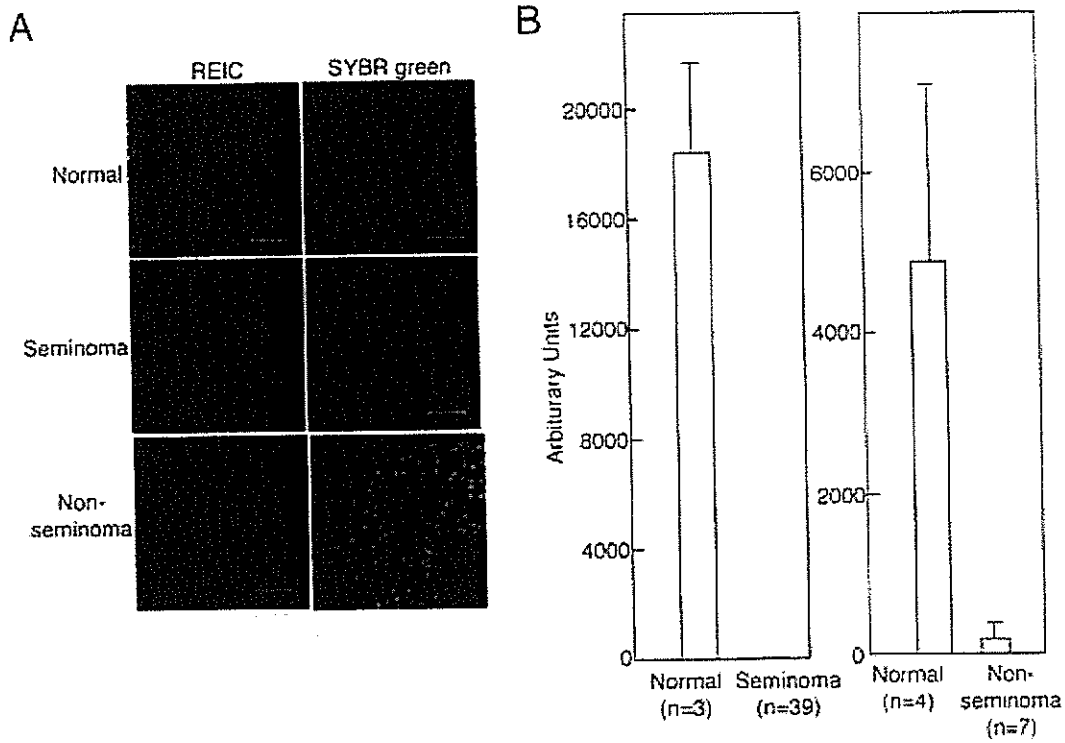

Figure 1. Expression of REIC/Dkk-3 in human seminoma and non-seminoma tissues. (A) Immunohistochemistry for REIC/Dkk-3 in representative normal testis and seminoma and non-seminoma tissues (red). Nuclei were visualized by staining with SYBR-Green. Scale bars: 200 μm for normal and seminoma tissues, 50 μm for non-seminoma tissue. (B) Quantitation of signals obtained by immunohistochemistry for REIC/Dkk-3. n, number of tissues analyzed; ordinate, arbitrary units; vertical bars, standard deviation.

from mixed germ cell tumor, was purchased from ATCC and maintained in RPMI-1640 supplemented with 10% fetal bovine serum. A c-Jun N-terminal kinase (JNK) inhibitor SP600125 was purchased from BioMol (Plymouth Meeting, PA).

Immunohistochemistry. Tissue sections and microarrays were immunostained with anti-human REIC/Dkk-3 antibody raised in our laboratory, followed by treatment with Alexa fluor R594-conjugated goat anti-rabbit IgG antibody (Molecular Probes, Eugene, OR). Vectashield mounting medium with DAPI (Vector Laboratories, Burlingame, CA) was used for counter-staining of cell nuclei. SYBR-Green I (Cambrex) was used for nuclear staining in tissue sections. The signal intensity of the stained samples was quantitated using the computer software Scion Image Beta (Scion, Frederick, ML).

RT-PCR. RT-PCR was performed under the conditions recommended by the manufacturer using a LightCycler™ rapid thermal cycler instrument (Roche Diagnostic, Lewes, UK). The primers used were as follows: REIC/Dkk-3 (forward) 5'-GTAAGTTCCCCTCTGGCTTG-3', REIC/Dkk-3 (reverse) 5'-AAGCACCAGACTGTGAAGCCT-3'; GAPDH (forward) 5'-GGGTGTGAACCATGAGAAGTATGA-3', GAPDH (reverse) 5'-TGCTAAGCAGTTGGTGGTGC-3'. The products were identified by a melting point analysis, electrophoretic mobility, and direct sequencing. Standard curves for calculation of the number of transcripts were made using plasmid containing the respective inserts. The results are shown as molar ratios of REIC/Dkk-3 to GAPDH transcripts

Western blot analysis. Western blot analysis was performed using protein extracts prepared at 48 h after infection of the adenovirus vectors. The antibodies used were as follows: rabbit anti-human REIC/Dkk-3 antibodies raised in our laboratory for REIC/Dkk-3; apoptosis sampler I kit (BD Biosciences, San Jose CA) for Bcl-2 and Bcl-xL; rabbit anti-human Bax antibody (Upstate Cell Signaling Solutions); mouse anti-horse cytochrome c antibody (Upstate Biotechnology, Lake Placid, NY); rabbit anti-human c-Jun antibody, rabbit anti-human phospho-c-Jun (Ser63) antibody, rabbit anti-human SAPK/JNK antibody, and rabbit anti-human phospho-SAPK/JNK (Thr183/Tyr185) antibody (Cell Signaling Technology, Beverly, MA); and mouse anti-human β-actin antibody (Sigma, St. Louis, MO).

Overexpression of REIC/Dkk-3 and monitoring of apoptotic cells. REIC/Dkk-3 was overexpressed by infecting cells with an adenovirus vector carrying REIC/Dkk-3 (Ad-REIC) described previously (16). A vector carrying LacZ (Ad-LacZ) was used as a negative control. Seventy-two hours after infection of the virus vectors at 20 MOI, apoptotic cells were monitored by TUNEL method using an *in situ* cell death detection kit (Roche).

In vivo experiments. NCCIT cells (3.0×10^6 in 50 μl PBS) were mixed with 50 μl Matrigel (BD Biosciences) and subcutaneously injected into the right flank of 8-week-old BALB/C nude mice (SLC, Hamamatsu, Japan). Three weeks after injection, when the tumor diameter reached ~5 mm,

$2.0x10^8$ pfu of Ad-REIC or Ad-LacZ in a 100 μl buffer were injected intratumorally. The size of the tumors was measured every 3 or 4 days for 30 days after the injection. Tumor volume was calculated using an empirical formula. V = 1/2 x (the shortest diameter)2 x (the longest diameter).

Results and Discussion

Reduced expression of REIC/Dkk-3 in testicular tumor tissues. We first examined the expression of the REIC/Dkk-3 gene in testicular tumor tissues. Immunostaining for REIC/Dkk-3 of a tissue microarray carrying 3 normal testicular tissues and 39 seminoma tissues showed that none of the seminoma tissues gave rise to any detectable signals while all the normal tissues were definitely positive for the expression (Fig. 1A). For non-seminoma cancer cases, clinically resected tissue samples were analyzed. All the non-seminoma tissues were negative in expression of REIC/Dkk-3. Quantitation of the signal intensity by computer software confirmed negative expression of REIC/Dkk-3 in both types of testicular cancer (Fig. 1B).

At present, the molecular mechanism of the reduced expression of REIC/Dkk-3 is not completely clear, although

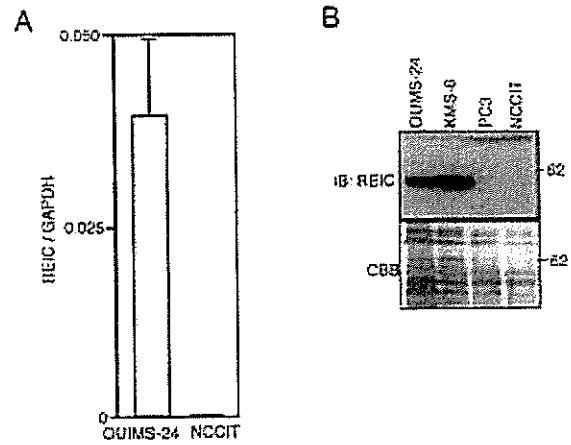

Figure 2. Reduced expression of REIC/Dkk-3 in a malignant human testicular germ cell cancer line, NCCIT. (A) Quantitative RT-PCR for REIC/Dkk-3 mRNA in normal human fibroblasts (OUMS-24) and NCCIT. Results were shown as molar ratios of REIC/Dkk-3 mRNA to GAPDH mRNA. (B) Western blot analysis for REIC/Dkk-3 protein in the designated cells. Normal human fibroblasts (OUMS-24 and KMS-6) and a human prostate cancer cell line (PC3) were used as positive and negative controls, respectively. CBB, stained with Coomassie Brilliant Blue.

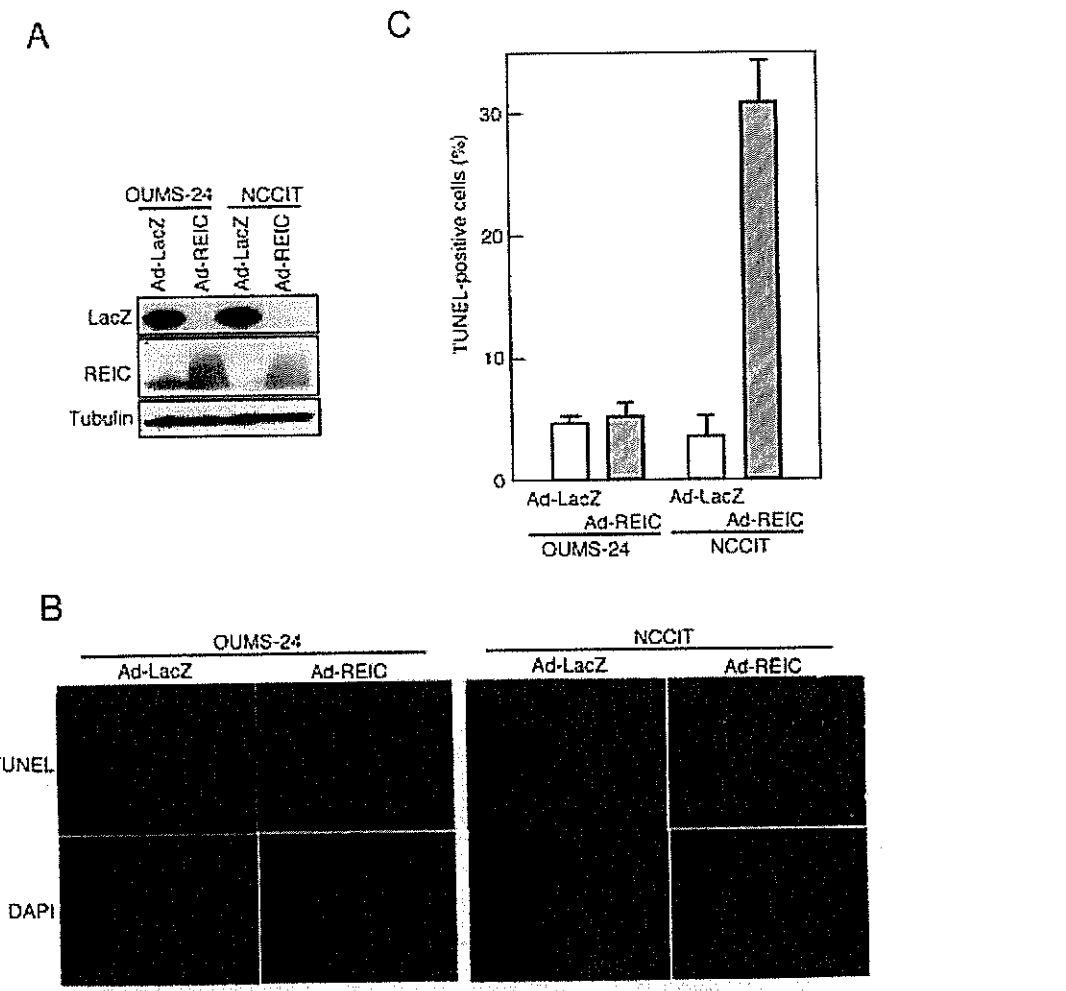

Figure 3. Induction of apoptotic cell death of NCCIT cells by overexpression of REIC/Dkk-3. (A) Overexpression of REIC/Dkk-3 or LacZ by an adenovirus vector. Cells were harvested 72 h after infection at 20 MOI for Western blot analysis. Tubulin was used as a control for applied amounts of protein. (B) TUNEL staining of cells 72 h after infection of the vectors at 20 MOI. Nuclei were visualized by DAPI staining. Scale bars, 200 μm. (C) Quantitation of the TUNEL-positive cells shown in B. Vertical bars, standard deviation.